24th International Conference on Renewable Energies and Power Quality (ICREPQ'26)
Santander (Spain), 10th to 12th June 2026
ISBN-13: 978-84-09-82044-3

MILP-Based Optimal Sizing of a Hybrid Battery-Hydrogen Energy Storage in a Grid-Connected Photovoltaic System

Zakaria A. Souleymane[1], A. Mpanda Mabwe[1], H. Augendre[2] and J. Fortin[1]

[1] UniLaSalle, GeNumEr, URR 7511, 80080 Amiens, France
Email: zakaria.souleymane@unilasalle.fr, augustin.mpanda@unilasalle.fr, jerome.fortin@unilasalle.fr

[2] BELLOVA, Aéroport Paris-Beauvais, CS 42158, 60000 Tillé, France
Email: herve.augendre@aeroportbeauvais.com

Abstract. This study is part of a large-scale decarbonization initiative for Paris-Beauvais Airport (PBA). The focus is the integration of renewable energy sources (RES) with the aim of decreasing grid dependency by enhancing local energy autonomy. The system under scrutiny comprises a photovoltaic (PV) generator, a Battery Energy Storage System (BESS), and a hydrogen energy storage subsystem ($\mathbf{H_2SS}$) consisting of an electrolyzer (ELZ), a hydrogen tank, and a fuel cell (FC). The global system supplies electrical loads and is connected to the utility grid. The sizing of the battery and hydrogen subsystems is determined by using a Mixed-Integer Linear Programming (MILP) model under realistic operational constraints. The system's operation is then evaluated through an explicit rule-based dispatch strategy, thereby enabling a clear interpretation of storage utilization over time.
The assessment of the framework employs three years of hourly load data, meticulously measured, and PV generation estimated from meteorological data. The results demonstrate the complementary roles of storage technologies: the battery mitigates short-term fluctuations, while hydrogen storage supports long-duration and seasonal balancing, and reduces grid dependency compared to a BESS-only configuration.
The proposed approach provides a realistic and interpretable basis for the design of hybrid storage systems in renewable-based infrastructures characterized by significant seasonal variability.

Key words. Optimal sizing, hybrid storage, battery, hydrogen, Mixed-Integer Linear Programming (MILP).

1. Introduction

In the current era, the decarbonization of infrastructure such as airports is of pivotal significance to the global energy transition, particularly through the large-scale integration of RES. Paris-Beauvais Airport (PBA) is contributing to this effort by initiating a project aimed at reducing its dependence on the national grid through the integration of Photovoltaic (PV), geothermal, and biomass energy into its energy mix. In accordance with the regulations outlined in Article 40 of France APER law (Acceleration of Production of Renewable Energies) **[1]**, which stipulates the installation of PV panels covering a minimum of 50% of the total surface area of parking facilities exceeding 1500 m², the project entails the implementation of solar car ports within the airport's parking infrastructure.

To reduce grid dependency and improve local energy autonomy within the PBA project, this work considers the use of a hybrid storage system consisting of battery and hydrogen storage.

It is evident from the findings of preceding studies that battery storage constitutes an effective solution in the short term, as evidenced by its high round-trip efficiency, high self-discharge rates and ability to respond quickly to power fluctuations **[2], [3]**.

In general, hydrogen has been identified as a potentially more viable solution for the purpose of long-term energy storage, primarily due to its capacity to accommodate substantial amounts of energy, in addition to its effectiveness in managing seasonal fluctuations inherent in renewable energy resources. Despite exhibiting lower round-trip efficiency when compared with alternative storage methods, hydrogen's notable advantage stems from its low self-discharge rates **[3]-[5]**.

A substantial number of studies have been conducted on hybrid systems combining batteries and hydrogen for energy management in renewable energy systems. These research studies principally focus on system sizing, optimization, and dispatch strategies using various approaches, such as mixed-integer linear programming (MILP) **[6], [7]**, and metaheuristic algorithms **[8]**. Other studies have relied on specialized software tools such as HOMER Pro **[9], [10]**.

Nevertheless, extant approaches do exhibit several inherent limitations. It is evident that certain studies have been conducted which utilize remarkably brief energy profiles – frequently a mere 24 hours or one month – that are then extrapolated to the annual time frame **[4], [11]**. This methodological decision, however, effectively hinders the capacity to accurately mirror the seasonal character of hydrogen storage. It is evident that other studies are predicated on a typical year, the construction or statistical representativeness of which is not delineated with sufficient detail **[6], [9]**. This limitation, consequent upon the imprecise nature of the underlying data, results in a concomitant restriction in the reproducibility of the results. It is evident that the majority of studies assess the performance of hybrid systems over a one-year period **[3], [8], [12]**. Nevertheless, this approach fails to account for interannual variability, potentially resulting in inaccurate sizing.

To address these limitations, the present article presents an analysis based on three full years of real data, enabling the seasonality of hydrogen storage to be explicitly represented, characterizing long-term storage events and quantifying inter-annual variability. The implementation of this approach enhances the reliability of the modelling and the robustness of the dimensioning of the hybrid system under scrutiny.

The structure of the remainder of the paper is as follows: Section 2 provides a detailed description of the methodological approach and the system modelling. In Section 3, the results of the study are presented, and a comparative analysis of the MILP is conducted. Finally, in Section 4, the study's conclusions and perspectives are outlined.

2. Methodology

A. System overview

The system under consideration H_2SS, illustrated in Fig. 1, consists of a photovoltaic (PV) generator, a battery energy storage system (BESS), and a hydrogen storage system (H_2SS). The latter consists of an electrolyzer (ELZ), a hydrogen tank and a fuel cell (FC). The system is responsible for supplying the load and is connected to the grid.

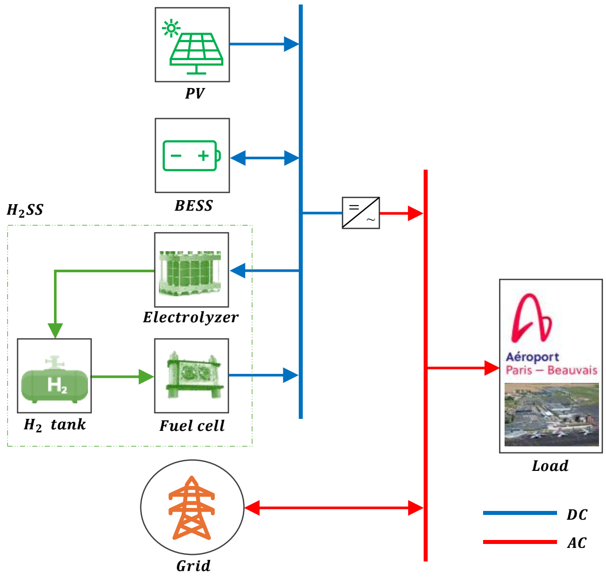

Fig. 1. Overview of the system under study

B. Data description

The study is conducted over a three-year period, with hourly resolution being employed to capture both short-term dynamics and seasonal variations in load demand and photovoltaic (PV) generation.

1) Load profile

The load profile is derived from real consumption data of the studied site over the period 2022-2024, with an hourly resolution. It captures both daily and seasonal demand variations. The corresponding profile is shown in Fig. 2.

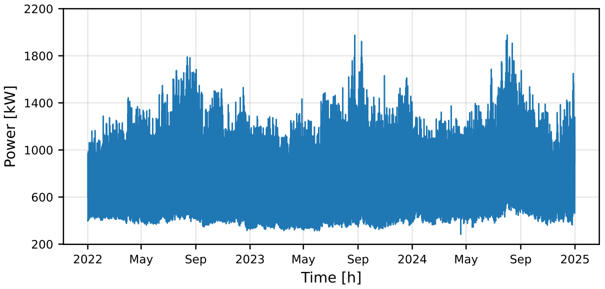

Fig. 2. Hourly load demand profiles of the airport (2022–2024).

2) PV generation

The PV generation is computed using an analytical model driven by plane of irradiance (POA) and cell temperature. The meteorological data which is required for this study is obtained from the ERA5 Reanalysis Dataset, which provides reliable hourly information. The POA is computed using the pvlib python library **[13]**, based on the Perez transposition model **[14]** which is based on the following factors: the panel tilt, the panel orientation and the solar position. The resulting PV power output is calculated as **[15]**:

$$P_t^{PV} = P^{STC} \cdot \frac{POA_t}{1000}\left(1 + \gamma(T_t^{PV} - 25)\right) \cdot N^{PV}, \forall t \in T \quad (1)$$

Where P^{STC} is the PV panel rated power at standard test conditions, γ is the power temperature coefficient, N^{PV} is the number of PV panel, T_t^{PV} is the cell temperature and is defined as:

$$T_t^{PV} = T_t^{amb} + POA_t * \frac{NOCT - 20}{800}, \forall t \in T \quad (2)$$

here T_t^{amb} is the ambient temperature and $NOCT$ is the nominal operating cell temperature.

The resulting PV generation profile is shown in Fig. 3.

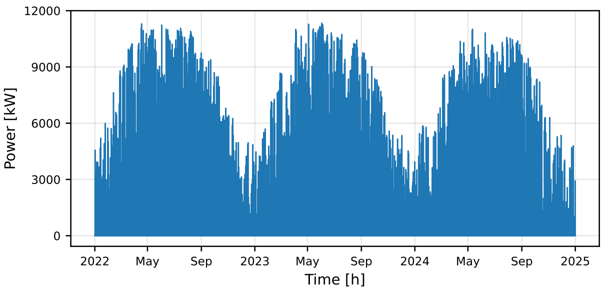

Fig. 3. Hourly PV generation profiles (2022–2024).

3) Electricity Price

The price of electricity is determined using day-ahead market data obtained from ENTSO [16], with hourly resolution. Fig. 4 illustrates the electricity price profile.

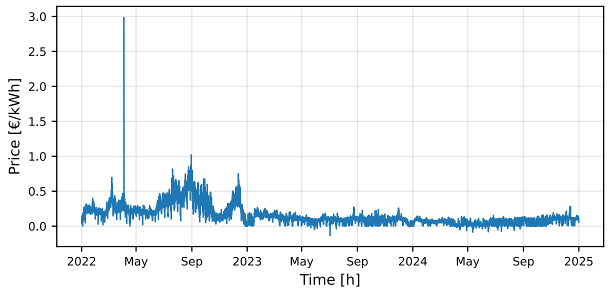

Fig. 4. Hourly Electricity price profile

C. *MILP-based sizing framework*

1) Objective function

In the planning stage, a MILP model is formulated with the purpose of determining the optimal sizing of the BESS and the H_2SS, including the BESS power rating and energy capacity, the ELZ and FC power rating, and the hydrogen storage capacity. The objective of the optimization problem is to minimize the total annualized cost, which is comprised of both investment (CAPEX) and operating (OPEX) costs (3).

$$min\ (CAPEX + OPEX) \tag{3}$$

The CAPEX accounts for the annual costs of the BESS and H_2SS components, and is expressed as:

$$CAPEX = CAPEX^{BESS} + CAPEX^{HSS} \tag{4}$$

With $$CAPEX^{BESS} = CRF_{r,l_P} \cdot C^P \cdot P^{BESS} + CRF_{r,l_E} \cdot C^E \cdot E^{BESS} \tag{5}$$

Where C^P and C^E are the unit investment costs associated with the power rating ($/kW) and energy capacity ($/kWh), respectively.

And $$CAPEX^{HSS} = CRF_{r,l_{ely}} \cdot C^{ely} \cdot P^{ely} + CRF_{r,l_{H_2}} \cdot C^{H_2} \cdot E^{H_2} + CRF_{r,l_{fc}} \cdot C^{fc} \cdot M_{H_2} \tag{6}$$

Where C^{ely} and C^{fc} are the unit investment costs associated with the power ratings ($/kW) of the ELZ and FC, respectively, and C^{H_2} is the unit investment cost of the hydrogen storage tank ($/kg).

The capital recovery factor (CRF) is used to annualize the investment cost, considering a discount rate r and equipment lifetime l_i. It is defined as:

$$CRF_{r,l_i} = \frac{r(1+r)^{l_i}}{(1+r)^{l_i} - 1} \tag{7}$$

The OPEX is defined as the total cost of purchased electricity, including both the grid charges and the penalties applied for load shedding, and is calculated by

$$OPEX = \frac{1}{N}\sum_t \left(C_t^{buy} \cdot P_t^{grid} + C^{shed} \cdot P_t^{shed}\right) \tag{8}$$

2) Decision between variables

The main decision variables are categorized as follows:

- Continuous variables

P_t^{ch}, P_t^{dis}: BESS charge and discharge power at time t

SoC_t: BESS state of charge at time t

P_t^{ely}, P_t^{fc}: ELZ and FC power at time t

H_t: Hydrogen tank level at time t

P_t^{shed}: Load shedding power at time t

P_t^{grid}: Grid power at time t

- Sizing variables

P^{BESS}, E^{BESS}: BESS Power rating and energy capacity

P^{ely}, P^{fc}: ELZ and FC power ratings

M_{H_2}: Hydrogen storage capacity

- Binary variables

u_t^{ch}, u_t^{dis}: Charging and discharging states of the BESS

u_t^{ely}, u_t^{fc}: ELZ and FC operating states

3) Constraints

The system is subject to a number of constraints, both operational and physical, with the purpose of ensuring power balance, BESS dynamics, and hydrogen storage dynamics.

The power balance of the system is given by:

$$P_t^{PV} + P_t^{dis} + P_t^{fc} + P_t^{grid} = P_t^{load} + P_t^{ch} + P_t^{ely} \tag{9}$$

The BESS and hydrogen storage dynamics are modelled through state-update equations and bounded operating limits. The BESS state of charge (SoC) and hydrogen storage level (H) are, respectively, given by:

$$SoC_{t+1} = SoC_t + \frac{\eta^{ch} P_t^{ch} - \frac{P_t^{dis}}{\eta^{dis}}}{E^{BESS}} \cdot \Delta t \tag{10}$$

$$H_{t+1} = H_t + \frac{\eta^{ely} P_t^{ely} - \frac{P_t^{fc}}{\eta^{fc}}}{M_{H_2}} \cdot \Delta t \tag{11}$$

Where η^{ch} and η^{dis} are respectively the BESS charge and discharge efficiencies. η^{ely} and η^{fc} are respectively ELZ and FC conversion factors.

Subject to:

$$SoC^{min} \leq SoC_t \leq SoC^{max} \tag{12}$$

$$H^{min} \leq H_t \leq H^{max} \tag{13}$$

$$0 \leq P_t^{ch} \leq u_t^{ch} \cdot P^{BESS} \tag{14}$$

$$0 \leq P_t^{dis} \leq u_t^{dis} \cdot P^{BESS} \tag{15}$$

$$0 \leq P_t^{ely} \leq u_t^{ely} \cdot P^{ely} \tag{16}$$

$$0 \leq P_t^{fc} \leq u_t^{fc} \cdot P^{fc} \tag{17}$$

$$u_t^{ch} + u_t^{dis} \leq 1 \tag{18}$$

$$u_t^{ely} + u_t^{fc} \leq 1 \tag{19}$$

4) Model parameters

The key technical and economic parameters employed in the MILP formulation and operational simulation are outlined in Table I.

Table I. Technical and economic parameters

Parameter	Value	Parameter	Value
T	3 years	Δt	1 hour
SoC^{min}	20%	SoC^{max}	80%
H^{min}	5%	H^{max}	95%
η^{ch}	91%	η^{dis}	91%
η^{ely}	0.0225 kg/kWh	η^{fc}	22.33 kWh/kg
C^{P}	255 €/kW	C^{E}	432 €/kW
C^{ely}	1 500 €/kW	C^{fc}	2 350 €/kW
C^{H_2}	450 €/kW	C^{shed}	100 €/kW
l_P	15 years	l_E	15 years
l_{ely}	15 years	l_{fc}	15 years
l_{H_2}	20 years	r	8%

The MILP model is implemented in Python 3.10.19 and solved using the CPLEX 22.1.2.0 optimization solver.

D. Rule-based operational dispatch

The optimal sizing results provide the foundation for the operational simulation of the system. A rule-based dispatch strategy is adopted to manage energy flows. The primary function of the PV generation is to satisfy the local demand. In scenarios where PV energy output exceeds requirements, the excess energy is then stored within the BESS until the state of charge attains its maximum limit. The resultant excess is then converted into hydrogen via an ELZ. In the event of an energy deficit, the battery is discharged to satisfy short-term demand. In instances where the battery has been depleted to its minimum charge level, hydrogen is utilized via the FC to facilitate the provision of energy to the load during protracted deficit periods. This strategy is indicative of a realistic operational policy, which in turn facilitates analysis of seasonal storage behavior. The corresponding control logic is outlined in algorithm 1.

Algorithm 1: Rule-based operational dispatch

for each time step t **do**
  if $P_t^{PV} \geq P_t^{load}$ **then**
    Supply the load using PV
    if $SoC_t < SoC^{max}$ **then**
      Charge the BESS
    else if $H_t < H^{max}$ **then**
      Run the electrolyzer
    else
      Curtail excess PV
    end if
  else
    if $SoC_t > SoC^{max}$ **then**
      Discharge the BESS
    else if $H_t > H^{max}$ **then**
      Run the fuel cell
    else
      Supply the load using the grid
    end if
  end if
end for

3. Results

A. Optimal sizing results

The optimal sizing results for the BESS-only and hybrid configurations are summarized in Tables II and III, respectively.

Table II. Optimal sizing results for the BESS-only configuration

Power rating [kW]	3 155.50
Energy capacity [kWh]	29 039.88

Table III. Optimal sizing results for the hybrid configuration

BESS	**Power rating [kW]**	2 841.31
	Energy capacity [kWh]	20 373.95
H_2SS	**Electrolyzer power rating [kW]**	1 536.67
	Fuel cell power rating [kW]	2 001.27
	Tank capacity [kg]	48 480.56

The findings indicate that the necessary battery capacity is substantially diminished in the hybrid configuration, while concomitantly, augmented capacity is assigned to the hydrogen storage system.
The disparities in dimensions are indicative of the repercussions of incorporating hydrogen storage within the system, thus prompting a subsequent examination of the consequent operational behavior.

B. Operational performance assessment

To evaluate the impact of the obtained sizing on system operation, a rule-based strategy is applied in order to simulate system behavior over the study period.

1) Aggregated energy balance over the study period
The energy balance over the three-year study period is summarized in Table III.

Table IV. Aggregated energy balance

	No storage	BESS	Hybrid
Load [MWh]	21 813.96	21 813.96	21 813.96
PV used [MWh]	10 670.26	19 153.40	21 813.96
Grid import [MWh]	11 143.70	2 660.56	0.00
PV curtailment [MWh]	34 246.15	23 961.05	18 661.46
Renewable share [%]	48.91	87.80	100.00

The findings indicate that energy storage has the capacity to augment the share of renewable energy, with an observed increase from 49.91% in the absence of storage to 87.80% with BESS and 100% with the hybrid system. Consequently, grid imports are observed to decrease significantly, with the hybrid configuration attaining near-complete load coverage. The results obtained provide a global assessment of system performance.

2) Monthly energy balance
To further analyze the temporal behavior of the system, a monthly assessment is conducted. As illustrated by Fig. 5 and Fig. 6, the monthly load demand is shown alongside the contribution of PV, BESS, FC, and the grid to the load supply. In addition, the associated PV curtailment for both the BESS-only and hybrid configurations is demonstrated.

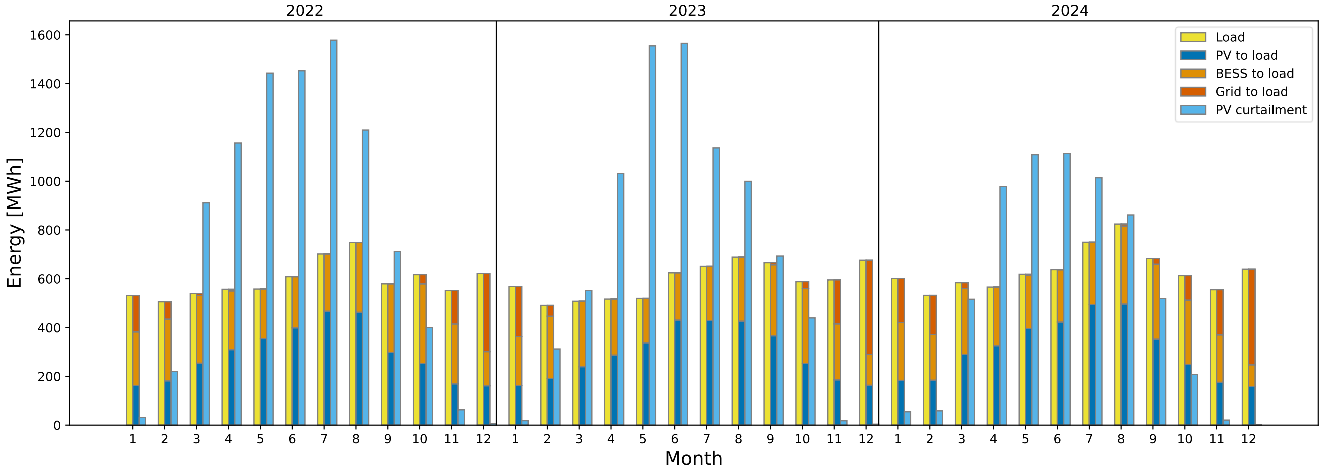

Fig. 5. Monthly load, supply allocation, and PV curtailment for BESS-only configuration

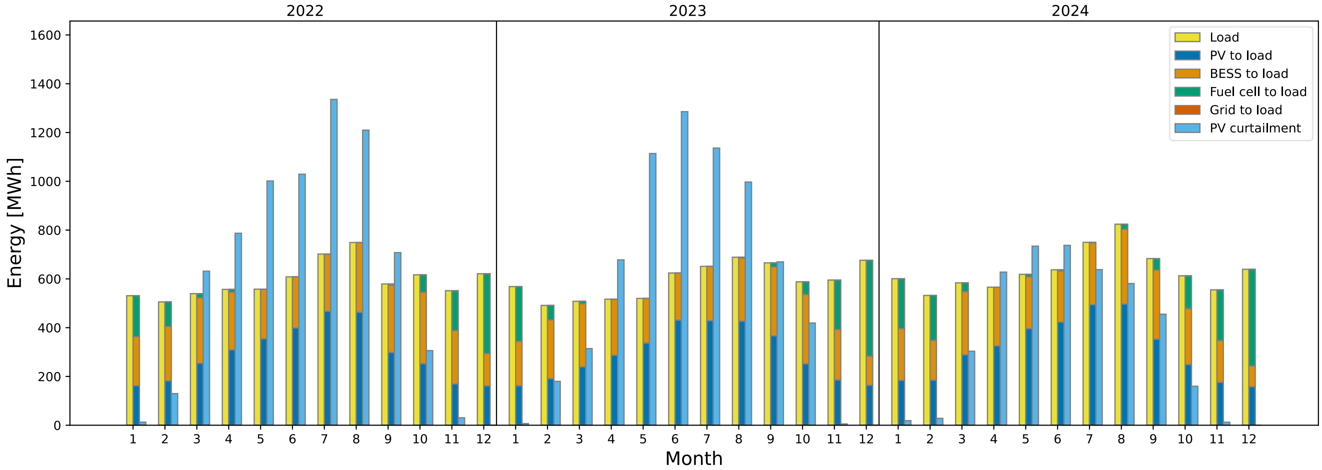

Fig. 6. Monthly load, supply allocation, and PV curtailment for hybrid BESS-Hydrogen configuration

As shown in Fig. 5 and 6, a discernible seasonal pattern is evident. In the BESS-only configuration, grid dependency increases during the winter months due to the limited long-duration storage capability. In contrast, the hybrid configuration enables H_2 storage to compensate for prolonged low-PV periods, thereby reducing grid imports and alleviating battery cycling. Moreover, the decline in PV curtailment signifies an enhancement in the RES utilization.

3) Dynamics of the Hybrid Storage System

To provide a more comprehensive interpretation of the observations, the temporal evolution of the BESS state of charge (SoC) and hydrogen storage level is analyzed and presented in Fig. 7.

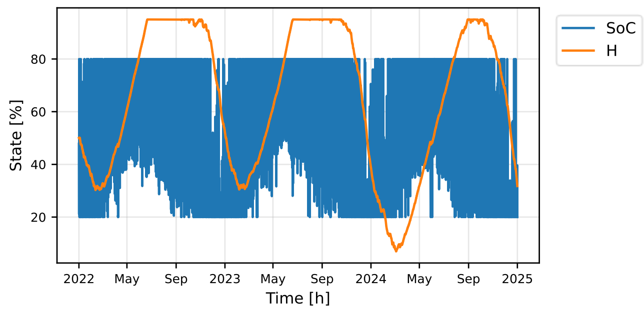

Fig. 7. State of charge of the BESS and hydrogen storage level

The BESS state of charge (SoC) displays frequent charge and discharge cycles, reflecting its active role in managing short-term fluctuations in PV generation and load demand. This rapid and dynamic process is indicative of its capacity to respond to transient imbalances and ensure immediate energy balancing within the system.

Conversely, the H_2 storage level evolves more gradually, indicating a slower dynamic associated with energy conversion and storage processes. In periods of surplus generation, the H_2SS accumulates energy, often reaching high levels. This behavior indicates that excess energy, which is unable to be accommodated by the BESS due to its limited capacity and operational constraints, is effectively directed towards long-term storage.

During extended deficit periods, the H_2 storage is gradually depleted, providing sustained energy support when the BESS alone is insufficient to meet demand. This delayed response is indicative of its function in addressing longer-duration energy imbalances as opposed to short-term fluctuations.

The observed dynamics demonstrate the differentiated temporal roles of the two storage systems. The BESS functions as a fast-response storage unit, while hydrogen storage provides enhanced flexibility for longer-duration energy management. This complementary interaction contributes to the enhancement of system adaptability and resilience during operation.

4. Conclusion

The present study investigates the optimal sizing and operation of a hybrid energy system integrating photovoltaic generation, battery storage, and hydrogen storage. A MILP-based optimization framework was developed to determine the optimal system sizing. Furthermore, a rule-based strategy was applied to evaluate system operation over a three-year period.

The findings indicate that the incorporation of H_2 storage substantially impacts system design, resulting in a decrease in the necessary battery capacity. The operational analysis demonstrates that combining short-term and long-term storage improves PV utilization and reduces grid dependency, with the hybrid configuration achieving near-complete load coverage over the study period.

The temporal analyses further highlight the complementary behavior of the two storage systems, whereby the BESS responds to short-term fluctuations, while H_2 storage contributes to the management of longer-duration energy imbalances. These findings confirm the relevance of integrating multi-timescale storage solutions to enhance the flexibility and performance of renewable-based energy systems.

Notwithstanding these enhancements, a considerable amount of PV curtailment persists under conditions of high generation. This unused energy underscores the potential for further optimization, particularly through the integration of flexible loads such as electric vehicle charging. In this context, the rapid growth of electric vehicles (EVs) offers a valuable opportunity to convert excess renewable generation into controllable demand or distributed storage via vehicle-to-grid (V2G) capabilities. It is recommended that future work consider the incorporation of forecasting techniques and uncertainty modelling with a view to enhancing the robustness of the proposed approach.

Acknowledgement

This work is supported by the Syndicat Mixte de l'Aéroport de Beauvais-Tillé (SMABT) and the Hauts-de-France Region.

References

[1] "Article 40 - LOI n° 2023-175 du 10 mars 2023 relative à l'accélération de la production d'énergies renouvelables (1) - Légifrance." Accessed: Feb. 13, 2026. [Online]. Available: https://www.legifrance.gouv.fr/loda/article_lc/LEGIARTI000052866747

[2] I. Gwayi, S. P. Ayeng'o, and C. Z. M. Kimambo, "Selection of electrochemical and electrical energy storage systems for off-grid renewable energy mini-grids: A review," *Cleaner Engineering and Technology*, vol. 25, p. 100906, Mar. 2025, doi: 10.1016/j.clet.2025.100906.

[3] S. Domene and S. Martin, "Exploration of the Trade-off between Short Term (Battery) and Long Term (Hydrogen) Storage for a Wind Powered Energy Community," in *2023 IEEE PES Innovative Smart Grid Technologies Europe (ISGT EUROPE)*, Oct. 2023, pp. 1–5. doi: 10.1109/ISGTEUROPE56780.2023.10408602.

[4] G. Jansen, Z. Dehouche, and H. Corrigan, "Cost-effective sizing of a hybrid Regenerative Hydrogen Fuel Cell energy storage system for remote & off-grid telecom towers," *International Journal of Hydrogen Energy*, vol. 46, no. 35, pp. 18153–18166, May 2021, doi: 10.1016/j.ijhydene.2021.02.205.

[5] X. Li, C. Jin, and Z. Wang, "Optimizing hybrid energy systems for renewable hydrogen production and storage with solar forecasting," *International Journal of Hydrogen Energy*, vol. 188, p. 151995, Nov. 2025, doi: 10.1016/j.ijhydene.2025.151995.

[6] M. Diabate, H. S. Krishnamoorthy, and J. Shi, "Optimal Hybrid Storage System Sizing to Provide Sustainable Energy to Subsea and Offshore Loads," in *2025 IEEE International Communications Energy Conference (INTELEC)*, Oct. 2025, pp. 132–137. doi: 10.1109/INTELEC63987.2025.11214767.

[7] X. Song, P. Gao, J. Zhang, C. Zhao, and Z. Zhang, "A comparative analysis of optimizing hydrogen and battery shared energy storage in hybrid power generation systems," *Applied Energy*, vol. 402, p. 127011, Jan. 2026, doi: 10.1016/j.apenergy.2025.127011.

[8] Y. Zhang, P. E. Campana, A. Lundblad, and J. Yan, "Comparative study of hydrogen storage and battery storage in grid connected photovoltaic system: Storage sizing and rule-based operation," *Applied Energy*, vol. 201, pp. 397–411, Sep. 2017, doi: 10.1016/j.apenergy.2017.03.123.

[9] P. Liu, S. K. Brika, K. M. Vagif, U. Yusupov, and Z. Jeang, "A hybrid decision-making framework for renewable-hydrogen energy storage integration: Enhancing economic and energy security," *International Journal of Hydrogen Energy*, vol. 144, pp. 482–495, Jul. 2025, doi: 10.1016/j.ijhydene.2025.05.222.

[10] M. Sarfraz, T. Xu, H. Meng, and R. Wang, "Techno-Economic Analysis of Hybrid Energy Storage Optimal Sizing in Self-Sufficient Renewable Energy System," in *2024 6th International Conference on Smart Power & Internet Energy Systems (SPIES)*, Dec. 2024, pp. 391–396. doi: 10.1109/SPIES63782.2024.10983619.

[11] E. Wöhr, D. Eser, M. Suriyah, and T. Leibfried, "Long-Term Power Management of a Building-Integrated DC Microgrid with Hybrid Energy Storage System in Grid-Connected Mode," in *2024 9th IEEE Workshop on the Electronic Grid (eGRID)*, Nov. 2024, pp. 1–6. doi: 10.1109/eGRID62045.2024.10842891.

[12] S. Jiang, S. Wen, M. Zhu, Y. Huang, and H. Ye, "Scenario-Transformation-Based Optimal Sizing of Hybrid Hydrogen-Battery Storage for Multi-Timescale Islanded Microgrids," *IEEE Transactions on Sustainable Energy*, vol. 14, no. 3, pp. 1784–1795, Jul. 2023, doi: 10.1109/TSTE.2023.3246592.

[13] W. F. Holmgren, C. W. Hansen, and M. A. Mikofski, "pvlib python: a python package for modeling solar energy systems," *Journal of Open Source Software*, vol. 3, no. 29, p. 884, Sep. 2018, doi: 10.21105/joss.00884.

[14] R. Perez, P. Ineichen, R. Seals, J. Michalsky, and R. Stewart, "Modeling daylight availability and irradiance components from direct and global irradiance," *Solar Energy*, vol. 44, no. 5, pp. 271–289, Jan. 1990, doi: 10.1016/0038-092X(90)90055-H.

[15] F. A. Kassab, B. Celik, F. Locment, M. Sechilariu, S. Liaquat, and T. M. Hansen, "Optimal sizing and energy management of a microgrid: A joint MILP approach for minimization of energy cost and carbon emission," *Renewable Energy*, vol. 224, p. 120186, Apr. 2024, doi: 10.1016/j.renene.2024.120186.

[16] "Transparency Platform." Accessed: Jan. 15, 2026. [Online]. Available: https://transparency.entsoe.eu/market/energyPrices